JOURNAL OF MATERIALS SCIENCE 32 (1997) 3951–3959

Non-destructive evaluation of porous MgO ceramics using acoustic techniques

T. KATHRINA*, R. D. RAWLINGS
Department of Materials, Imperial College of Science, Technology and Medicine, Prince Consort Road, London SW7 2BP, UK

Two acoustic techniques, ultrasonics (US) and acousto-ultrasonics (AU), were used to evaluate MgO extrudate in both the green and sintered states. In US, the velocity was measured and in AU ringdown counts, pulse amplitude, pulse width and spectrum were used to quantify the output signal. The acoustic measurements showed good reproducibility, especially velocity. Under some sintering conditions the ultrasonic velocity and the porosity were lower than in the green state: this was attributed to pore growth in the early stages of sintering. It was found that as the temperature and time of sintering increased, the density, compressive strength and ultrasonic velocity increased. However, the response of the AU parameters to changes in sintering conditions was more complex, for example, the peak amplitude increased whereas pulse width and ringdown counts decreased with increasing temperature of sintering. The US and AU data on the sintered MgO extrudate were correlated with the structure and properties. Empirical relationships between the acoustic parameters and porosity and compressive strength were obtained which gave better coefficients of regression for the ultrasonic velocity than for acousto-ultrasonic parameters. It was concluded that US, and in some instances AU, are feasible as quality control techniques/non-destructive evaluation for ceramics.

1. Introduction

Ceramic materials are, in general, hard, wear and corrosion resistant and can withstand high stresses at elevated temperatures. The advantages of structural ceramics, however, are somewhat offset by the fact that they are brittle; consequently, very small defects can lead to a dramatic decrease in their strength. These defects, therefore, must be detected before the catastrophic failure of the structure occurs.

Non-destructive evaluation (NDE) techniques, which by definition do not damage the component under inspection, are required to evaluate this important class of materials. The objective of most NDE for ceramic materials is the detection of cracks, porosity, inclusions, and other features that affect the properties of the components [1].

The use and potential offered by ultrasonic (US) and acousto-ultrasonic (AU) techniques as NDE methods as a mean of controlling the quality of ceramic products, are being explored. US techniques involve measuring either ultrasonic velocity or attenuation of materials, and previous reports include studies of ceramics during compaction [2, 3], in the green state [4, 5], during drying, sintering and cooling [6] and after sintering [7].

AU techniques combine advantageous aspects of acoustic emission (AE) and US methodologies and alleviate some of their weaknesses; the US method is not very sensitive to high attenuated materials and dispersed flaws, and the stress required for AE may damage the structure of the materials. AU consists of introducing a repeating series of ultrasonic pulses into the material under test and quantifying the output waveform using AE methods. The output waveform is quantized in terms of the "stress wave factor" (SWF) which is defined as a relative measure of the efficiency of energy dissipation in a material [8]. If flaws or other material anomalies exist in the volume being examined, their combined effect will be reflected in the SWF. The SWF in its simplest form may be evaluated as a ringdown count, peak-amplitude distribution and pulse width, which are the basic parameters used in quantifying an AE signal. AU studies on brittle materials, e.g. alumina, glass and glass ceramic, have been previously made and the AU data correlated with the structure and microcracking [2, 3, 9–12].

This paper reports the use of acoustic NDT techniques, namely US and AU, for the characterization of MgO extrudate in the green and sintered states. The US (ultrasonic velocity) and AU (ringdown counts, peak amplitude and pulse width) data are correlated with the measured physical (density and porosity) and mechanical (compression strength) properties in order to determine the feasibility of employing these techniques as NDE methods for this type of ceramic material.

* *Present address*: P3FT-LIPI, Komplex PUSPIPTEK, Serpong, Tangerang 15314, Indonesia

0022–2461

2. Experimental procedure

Porous cylindrical MgO extrudate rods, used for heating elements, of diameter $\cong 6.6$ mm and length $\cong 46$ mm with four parallel longitudinal holes, were supplied in the green state and after sintering at 1320 °C for 3 h by Morgan Materials Technology Ltd. The green samples were then sintered for different temperatures and times (some at temperature in the range 1200–1450 °C for 1 h and 3 h, and others for between 1 and 20 h at 1200 or 1350 °C) at Imperial College (IC), to investigate the dependency of US and AU parameters and material properties on sintering conditions. These sintering conditions were chosen to produce a wide range of porous (26%–32% porosity) samples for examination.

The acoustic set-up was based on Dunegan/Endevco 3000 Series Acoustic Emission equipment and is illustrated in Fig. 1. The ceramic rod sample was placed between the broad-band ultrasonic transducers (frequency range 175–1000 kHz). Dry couplant, a thin piece of vinyl material, was used to achieve a good contact between the transducers and the sample and to avoid the contamination of porous ceramics that occurs when wet couplants are employed [10]. Owing to the dependency of acoustic measurement on the contact pressure between the transducer and sample, a constant pressure was applied for all measurements by the use of a constant load spring which was mounted inside the transducer holder. An ultrasonic pulse from the transmitter was generated, passed through the rod sample and detected by the second transducer acting as a receiver. The output signal was recorded and quantified in terms of ringdown counts (RDC), peak amplitude (PA) and pulse width (PW). In addition, the waveform and its spectrum were recorded for ultrasonic velocity measurement and spectrum analyses, respectively.

The ultrasonic velocity was obtained by measuring the travel time, t, of ultrasonic waves through the rod sample. Knowing the sample length, s, the ultrasonic velocity, v, of the ceramic sample was obtained from

$$v = \frac{s}{t} \tag{1}$$

A total gain of 80 dB (preamplification of 40 dB), a threshold of 30 dB, an envelope of 100 μs, and an input pulse of constant energy at a rate of 1 Hz were used throughout the work. A single reading was cumulated for 50 input pulses. To reduce errors associated with slight variations in test conditions, such as constant pressure and contact area, readings were repeated ten times for each sample by lifting up the holder and replacing it after turning the sample through about 36°. Mean values for RDC, PA and PW were then calculated.

After the acoustic measurements, the rods were cut transversely to give cylindrical specimens 12 mm in length which were tested in compression using a Nene mechanical tester operating at a crosshead speed of 0.25 mm min^{-1}. The compressive strength was determined by dividing the fracture force by the load-bearing area of the sample, i.e. the cross-sectional area of the rod minus the cross-sectional area of the four holes.

The density, ρ, of the samples was evaluated from the mass in air and the volume as determined from dimensions (length and diameter of rod by micrometer and hole diameters by a calibrated light microscope). The porosity of a sample, p, was obtained from the density using

$$p = \left(1 - \frac{\rho}{\rho_{MgO}}\right) \times 100\% \tag{2}$$

where ρ_{MgO} is the density of MgO taken to be 3.58 Mg m^{-3} from the literature [13].

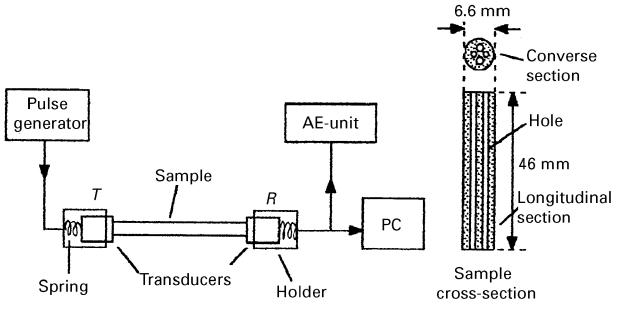

Figure 1 Diagram of the arrangement for acoustic testing and of the MgO sample.

3. Results and discussion

3.1. Physical properties

The density of samples sintered for 1 or 3 h at, or below, 1400 °C was less than the density in the green state (Fig. 2). The density increased with increasing sintering temperature, and the density of the samples sintered at, or above, 1400 °C exceeded that of the green state. The density of the samples sintered for 3 h was always greater than that of those sintered for 1 h. The density of as-received sintered samples (designated Morgan) was close to the value for samples sintered at Imperial College.

Results of sintering for different times (1–20 h) at 1200 and 1350 °C showed that the density increased

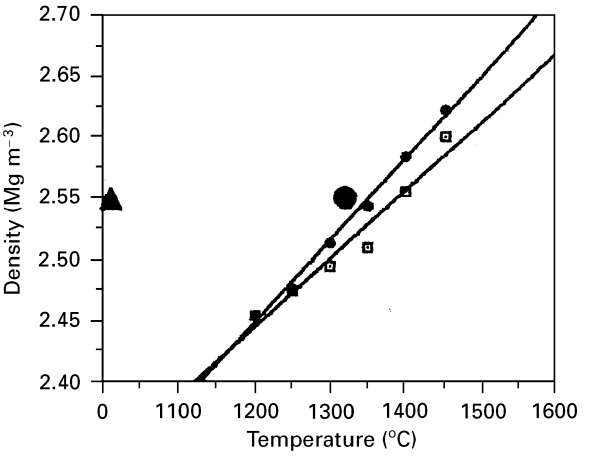

Figure 2 Effect of sintering temperature on density (sintering times of (⊡) 1 and (●) 3 h). Data for the as-received green (▲, Green) and sintered (●, Morgan) samples are also included.

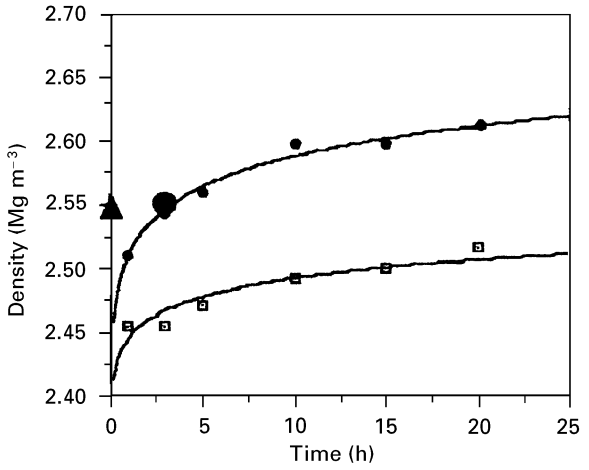

Figure 3 Effect of sintering time on density (sintering temperatures of (⊡) 1200 and (●) 1350 °C). Data for the as-received green (▲, Green) and sintered (●, Morgan) samples are also included.

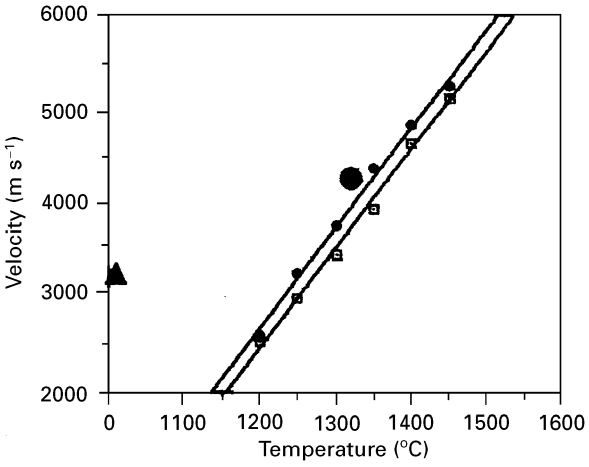

Figure 4 Effect of sintering temperature on velocity (sintering times of (⊡) 1 and (●) 3 h). Data for the as-received green (▲, Green) and sintered (●, Morgan) samples are also included.

logarithmically with time (Fig. 3). At 1200 °C the density remained below the density of the green state (even after 20 h), whereas at 1350 °C a sintering time of 5 h was sufficient to increase the density over that of the green state. The decrease in density from the green value observed with some of the sintering conditions is attributed to pore growth in the early stages of sintering [14].

3.2. Ultrasonic velocity

Ultrasonic velocity measurements were reproducible to within 1.5%. A linear relationship was obtained between ultrasonic velocity and sintering temperature (Fig. 4). The slope was the same for the plots for 1 and 3 h sintering but with the higher velocities exhibited by the samples that had undergone the longer heat treatment. Fig. 5 also shows that the velocity increased with increasing sintering time and that the relationship was logarithmic. The time and temperature dependencies of the velocity are thus similar to those of density. This is fortuitous as v is an inverse function of density and is also function of Young's

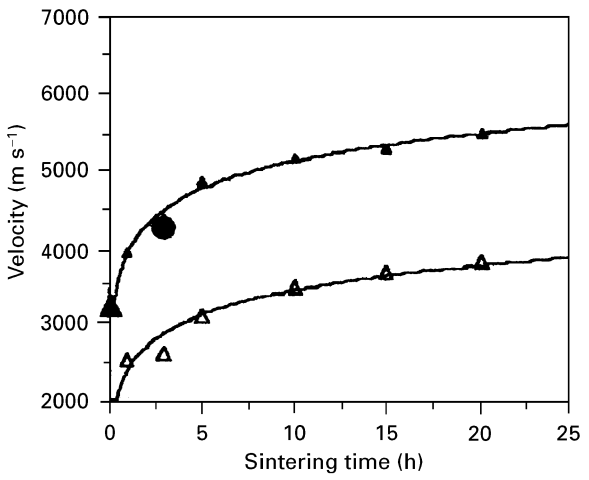

Figure 5 Effect of sintering time on velocity (sintering temperatures of (△) 1200 and (▲) 1350 °C). Data for the as-received green (▲, Green) and sintered (●, Morgan) samples are also included.

modulus, E, according to

$$v = \left(\frac{E}{\rho}\right)^{1/2} \tag{3}$$

It is well established that E falls with decreasing porosity. A number of expressions may be found in the literature for the porosity dependence of E, and all indicate that E is sensitive to porosity changes. In comparison, ρ is less sensitive to porosity. Hence the pore growth that is considered to have occurred under certain sintering conditions, and that led to a reduction in density with respect to the green density, also produced a decrease in velocity through the dominating effect of the decrement in E. The positive dependencies of velocity on time and temperature may be accounted for by the improved bonding between particles and the reduction in porosity that is a consequence of sintering; these result in higher moduli values which outweigh the adverse effect on v of the increase in density.

3.3. Acousto-ultrasonic

AU measurements were reproducible to within less than 10%; even though the reproducibility of this technique was not as good as the ultrasonic velocity measurement, it was worthy of further investigation as a quality control method. Indeed, US measurements complemented with AU measurements may sometimes give a fuller characterization.

The temperature dependence of the AU parameters differed; the PA increased linearly with increasing temperature (Fig. 6) whereas the RDC and PW exhibited a negative linear temperature dependence (Figs 7 and 8). These trends may also be seen in the waveforms (Fig. 9). Similar opposite trends for PA and RDC/PW were observed as a function of sintering time, e.g. at 1200 °C PA increased and RDC and PW were approximately constant with time, but at 1350 °C PA was approximately constant (Fig. 10) and RDC and PW decreased as exemplified by the plots for pulse width in Fig. 11.

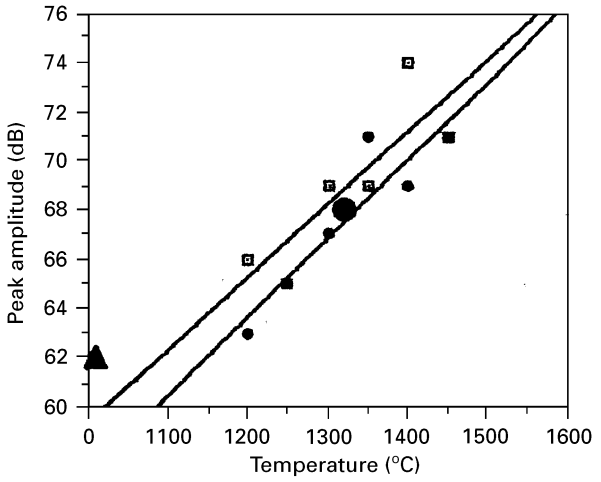

Figure 6 Effect of sintering temperature on pulse amplitude (sintering times of (⊡) 1 and (●) 3 h). Data for the as-received green (▲, Green) and sintered (●, Morgan) samples are also included.

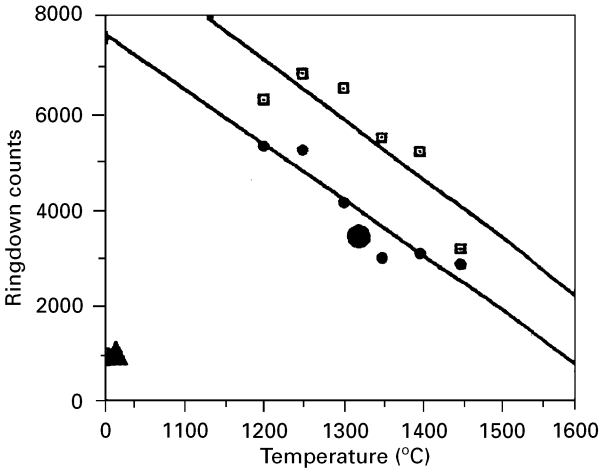

Figure 7 Effect of sintering temperature on ringdown count (sintering times of (⊡) 1 and (●) 3 h). Data for the as-received green (▲, Green) and sintered (●, Morgan) samples are also included.

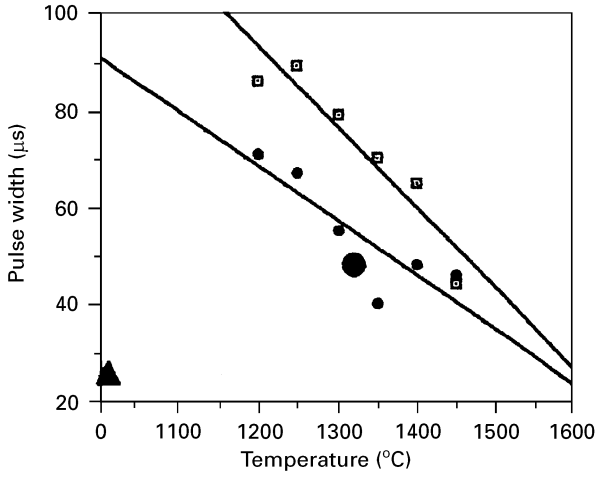

Figure 8 Effect of sintering temperature on pulse width (sintering times of (⊡) 1 and (●) 3 h). Data for the as-received green (▲, Green) and sintered (●, Morgan) samples are also included.

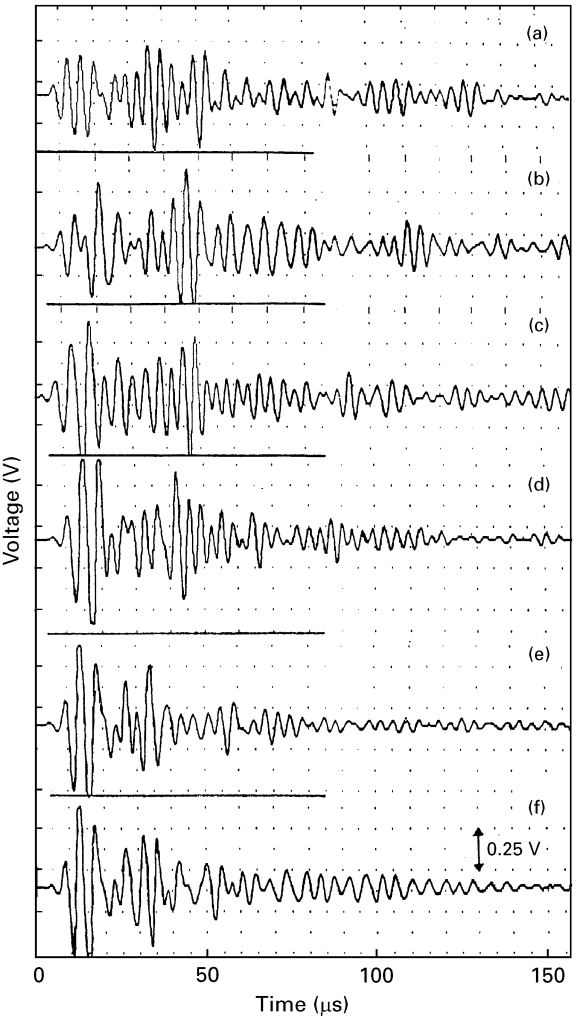

Figure 9 The waveform of the output signal as a function of sintering temperature (constant sintering time of 3 h): (a) 1200 °C, (b) 1250 °C, (c) 1300 °C, (d) 1350 °C), (e) 1400 °C, and (f) 1450 °C.

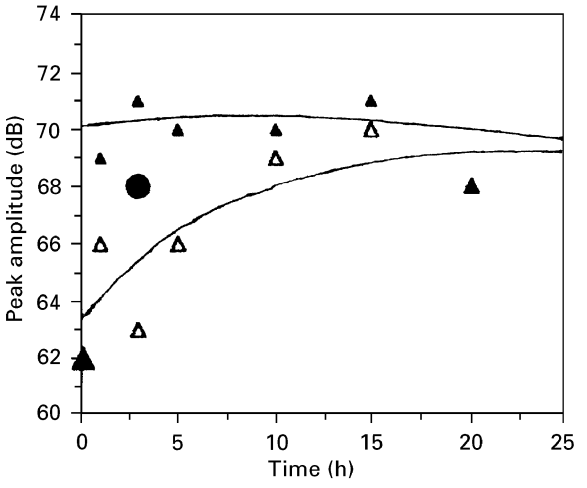

Figure 10 Effect of sintering time on pulse amplitude (sintering temperatures of (△) 1200 and (▲) 1350 °C). Data for the as-received green (▲, Green) and sintered (●, Morgan) samples are also included.

Many factors influence a propagating wave as it interacts with the microstructure, and previous work has indicated that the AU parameters are more sensitive to the fine details of the microstructure than the acoustic velocity [10, 15, 16]. Acoustic wave propagation is complex and involves the effects of different wave types, mode conversion and reflection, attenuation and dispersion. The effects of attenuation and

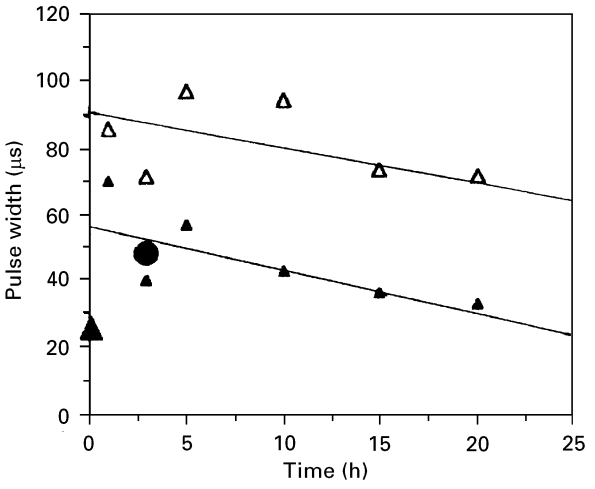

Figure 11 Effect of sintering time on pulse width (sintering temperatures of (△) 1200 and (▲) 1350 °C). Data for the as-received green (▲, Green) and sintered (●, Morgan) samples are also included.

dispersion are to degrade the signal, hence slowing down the rise time, increasing the pulse length and depressing the amplitude [17]. Vary [18] also stated that PA was an inverse function of attenuation. Sintering is enhanced by increasing the temperature and, to a lesser extent, by increasing the time, of sintering and the improved inter-particle bonding and decrease in porosity results in a fall in attenuation. This accounts for the general trends observed in the present investigation of increasing PA and decreasing PW as the degree of sintering increases, i.e. as the temperature or time of sintering is increased.

The RDC from a pulse depends on the amplitude and the width; a high amplitude leads to high counts and a small width favours low counts. In the present case, the temperature and time dependencies of RDC indicate that the count was dominated by the changes in PW rather than PA (see, for example, the similar trends shown in the data of Figs 7 and 8).

The waveforms (Fig. 9) are the result of a highly modulated complex output signal consisting of numerous superimposed wavelets. It can be seen that as the degree of sintering improved with increasing temperature, so the number of wavelets scattered by pores was reduced (fewer sub-pulses in the signal). Again this is consistent with both RDC and PW decreasing with increasing sintering temperature.

Spectrum analysis was also used to analyse the output signal and was found to be capable of differentiating between samples sintered at different temperatures. The spectra for samples sintered at temperatures in the range 1200–1450 °C for 3 h are shown in Fig. 12. A number of modifications to the spectra occur with increasing sintering temperature, namely a decrease in the number of peaks from seven to five, a decrease in the background and peak overlap, and a change in the relative intensities of the peaks. These results are in agreement with the finding of Aduda and Rawlings on sintered glass systems [15, 16]. They concluded that the multiplicity of peaks in the frequency spectra is due to defects (pores, crack, etc.) which interfere with the ultrasonic waves, in a manner analogous to Bragg interference, and cause time delays owing to scattering. Thus the lower the defect content, in the present case porosity, the fewer are the peaks with less overlap.

3.3.1. Compressive strength

In common with other brittle materials, the result of the compressive strength measurements showed considerable scatter; nevertheless it is clear from the figures (Figs 13 and 14) that the compressive strength increased with increasing temperature and time sintering.

3.4. Relationships between acoustic parameters, porosity and compressive strength

The definition of an NDE technique is that it does not degrade the performance of a component, so that a component, if judged to be in a satisfactory condition, may be put back into service. Clearly there is a distinct advantage in NDE testing and currently there is considerable interest in correlating data from NDE and destructive testing such as mechanical testing. Once the interrelation between these techniques is established for a certain application, then NDE methods, which are often rapid, can be used for quality control instead of destructive techniques [19] and hence improve efficiency and give economic benefits.

In the current work, correlations between acoustic NDE and physical (porosity) and mechanical (compressive strength) properties were made for the sintered MgO extrudate using a standard curve-fitting programme. Results from the as-received green and sintered samples were not included in the curve fitting, but data for these samples have been plotted on the graphs to see the degree of fit to the curves.

3.4.1. Relationship between ultrasonic velocity, porosity and strength

A straight-line correlation with a coefficient of regression of 0.97 was found between ultrasonic velocity and porosity (Fig. 15) over the porosity range of 26%–32% studied in the present work

$$v_p = v_0 - ap \tag{4}$$

where v_p is the velocity at porosity p, v_0 is the zero porosity velocity (22 000 m s^{-1}) and a is a constant (603). It can be seen that the sintered as-received sample (Morgan) result is on the correlated straight line, whereas the result from the green sample (Green) lies below the curve.

On the other hand, Phani *et al.* [9] showed that the relationship between ultrasonic velocity and porosity may be described by the equation

$$v = v_0(1 - p)^m \tag{5}$$

where m is a constant. Plotting $\ln(v)$ versus $\ln(1 - p)$ for the present data gave a linear correlation with a coefficient of regression of 0.947, $v_0 = 162\,755$ m s^{-1}, and $m = 11$ (Fig. 16).

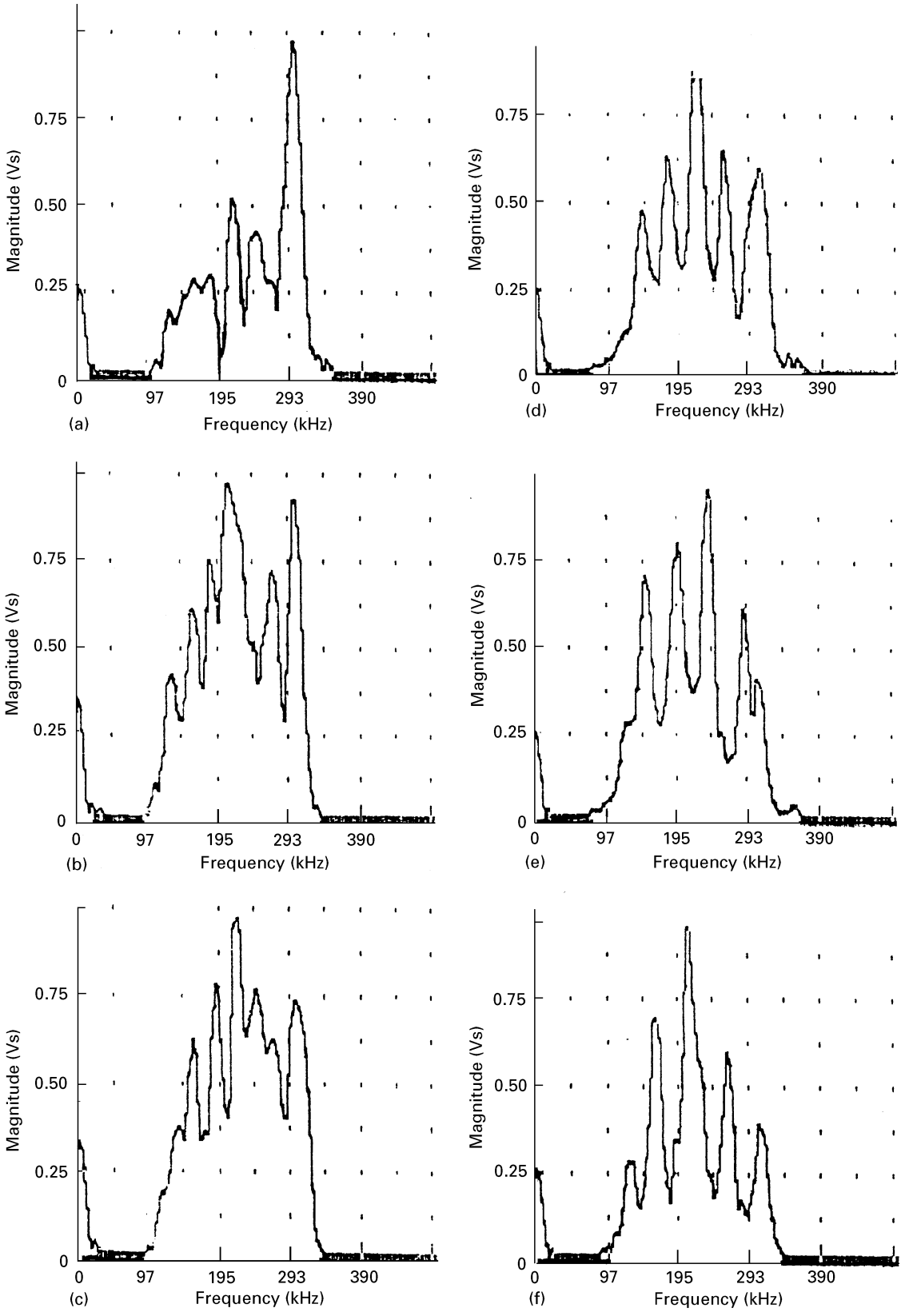

Figure 12 Spectrum of the output signal as a function of sintering temperature (constant sintering time of 3 h): (a) 1200 °C, (b) 1250 °C, (c) 1300 °C, (d) 1350 °C), (e) 1400 °C, and (f) 1450 °C.

The values of v_0 from both the above equations are very high compared to the literature value of 5770 $m\,s^{-1}$ [20], indicating the above correlations are not applicable at low porosities. However, both equations give a good fit over the porosity range (26%–32%) of the investigation.

The relationship between ultrasonic velocity and compressive strength, σ_c, over the wide range of compressive strengths (10–450 MPa) exhibited by the samples was logarithmic (Fig. 17)

$$v_{st} = v_0 + b \log \sigma_c \quad (6)$$

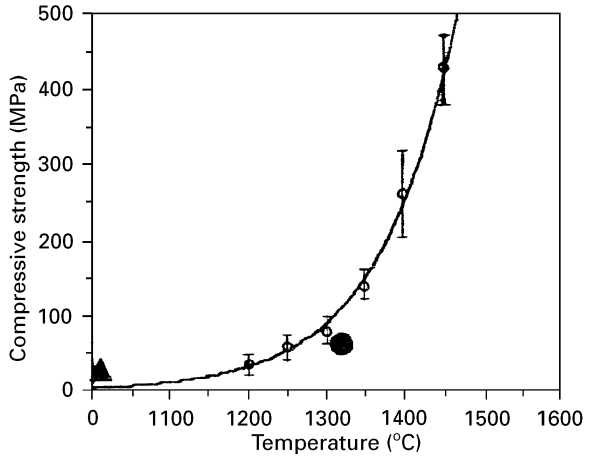

Figure 13 Effect of sintering temperature on compressive strength (sintering time of (○) 1 h). Data for the as-received green (▲, Green) and sintered (●, Morgan) samples are also included.

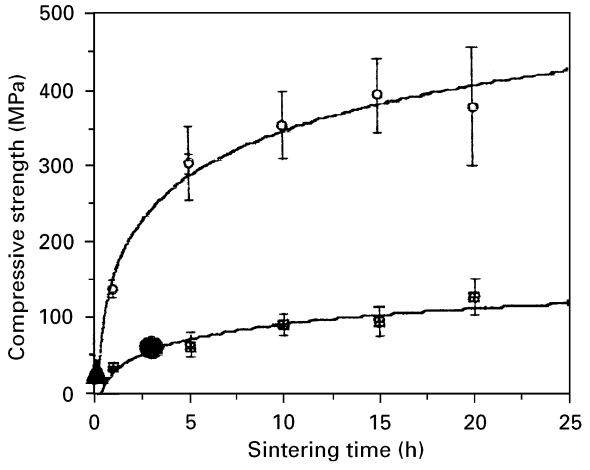

Figure 14 Effect of sintering time on compressive strength (sintering temperatures of (⊞) 1200 and (○) 1350 °C). Data for the as-received green (▲, Green) and sintered (●, Morgan) samples are also included.

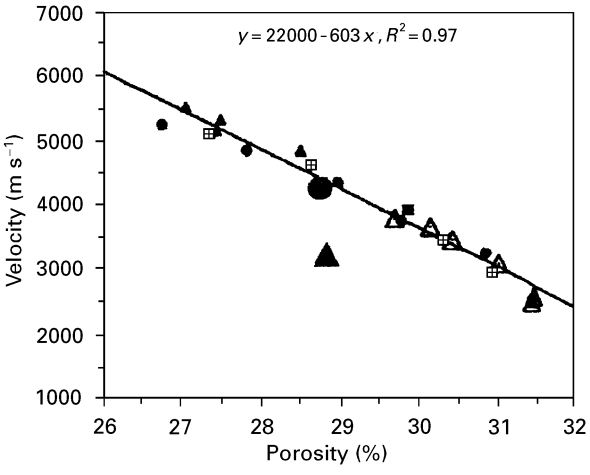

Figure 15 Plot showing a linear relationship between velocity and porosity for MgO extrudate sintered for different times and temperatures: (⊞) 1 h, (●) 3 h, (△) 1200 °C, (▲) 1350 °C; (▲) Green, (●) Morgan.

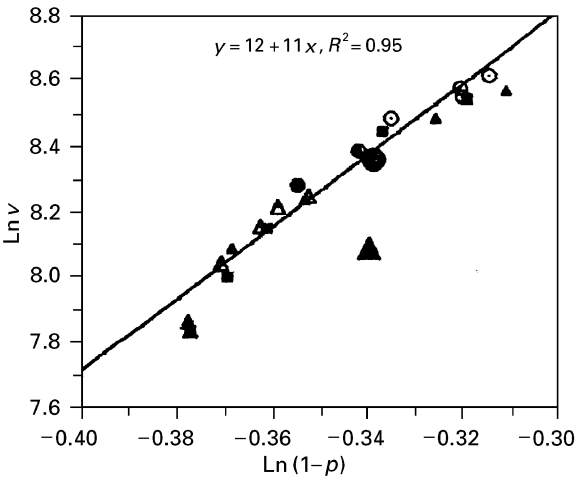

Figure 16 Plot in ln(velocity) against ln(1 − *p*), where *p* is porosity, for MgO extrudate sintered for different times and temperatures in accordance with the equation due to Phani *et al.* [7]. (■) 1 h, (▲) 3 h, (△) 1200 °C, (⊙) 1350 °C; (▲) Green, (●) Morgan.

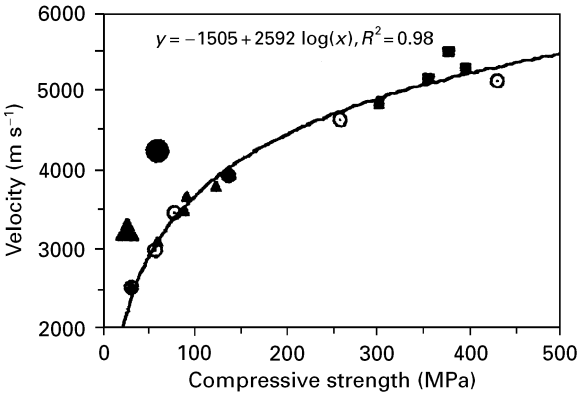

Figure 17 Plot showing a logarithmic relationship between velocity and compressive strength or MgO extrudate sintered for different times and temperatures: (⊙) 1 h, (▲) 1200 °C, (■) 1350 °C; (▲) Green, (●) Morgan.

where v_{st} is the velocity at compressive strength σ_c, v_0 is the velocity ($-1505\ m\ s^{-1}$) when $\sigma_c = 1$, b is a constant (2592) and the coefficient of regression is 0.98. Clearly, the value for v_0 has no physical meaning. The values of the as-received samples were found to fit closely the above correlation.

These correlations demonstrate that velocity measurements may be employed to estimate the porosity and compressive strength of porous MgO. For example, the velocity may be measured to within 1.5% which gives a possible error of typically 5%–7% in the predicted compressive strength; this error is less than the experimental variation in the compressive strength values.

3.4.2. Relationship between acousto-ultrasonic parameters, porosity and strength

Both PW and RDC show a linear relationship with porosity, *p*, with coefficients of regression of 0.74 and 0.73, respectively (see, for example, the plot for RDC

in Fig. 18)

$$PW = PW_0 + ep \quad (7)$$

$$RDC = RDC_0 - fp \quad (8)$$

where subscript 0 refers to the values at zero porosity (-255 μs and -24400) and e and f are constants with values of 10.9 and 997, respectively.

In contrast, a polynomial with an order of 2 gave the best correlation for the porosity dependence of PA (Fig. 19)

$$PA = PA_0 + cp + dp^2 \quad (9)$$

where PA_0 is the peak amplitude at zero porosity (-441 dB), c and d are constants (36 and 0.6, respectively) and the coefficient of regression is 0.69.

Two points arise from these equations. The first is that the values for the parameters at zero porosity (PA_0, PW_0 and RDC_0) are all negative, and therefore have no physical meaning. Thus the relationships do not apply at low porosities. The second point is that the coefficients of regression are much lower than for the equivalent velocity–porosity relationships. This is considered to be a consequence of the AU parameters being more sensitive than velocity to microstructure. The AU parameters depend not only on the percentage porosity but also on other microstructural features such as the size and shape of the pores, e.g. the larger the pore size the greater is the attenuation and the lower are the AU parameters [10, 15]. It follows that estimates of porosity from AU data are unlikely to be as good as those from velocity measurements.

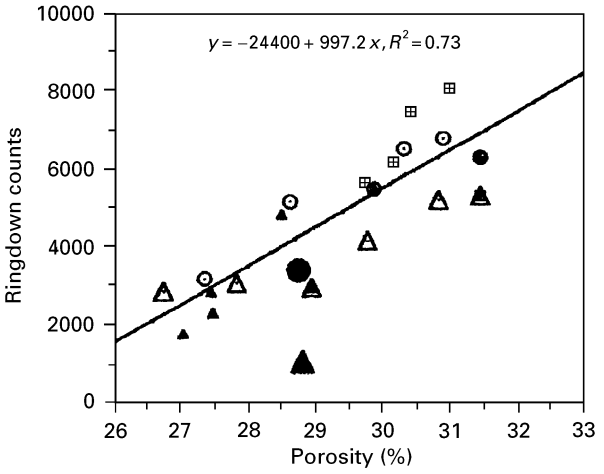

Figure 18 Plot showing a linear relationship between ringdown count and porosity for MgO extrudate sintered for different times and temperatures: (⊙) 1 h, (△) 3 h, (⊞) 1200 °C, (▲) 1350 °C; (▲) Green, (●) Morgan.

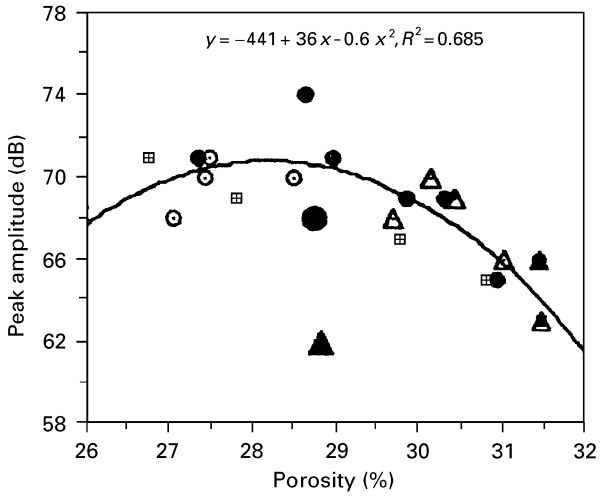

Figure 19 Plot showing a polynomial relationship between pulse amplitude and porosity for MgO extrudate sintered for different times and temperatures: (●) 1 h, (⊞) 3 h, (△) 1200 °C, (⊙) 1350 °C; (▲) Green, (●) Morgan.

The best fit equations relating AU parameter to compressive strength were

$$PA = 59.4 + 4.5\log \sigma_c \quad (10)$$

$$PW = 94 - 0.14\ \sigma_c \quad (11)$$

$$RDC = 7611 - 12.4\ \sigma_c \quad (12)$$

with coefficients of regression of 0.49, 0.88 and 0.84, respectively. These coefficients of regression are again lower than for the equipment velocity correlations. Nevertheless, the linear relationships with reasonable coefficients of regression for PW and RDC are encouraging, especially the latter, as ringdown counting is the simplest AU analysis method. A 5% variation in RDC will give an uncertainty of between 3% and 20% in the predicted strength.

4. Conclusion

Ultrasonic (US) and acousto-ultrasonic (AU) techniques have been used to characterize the green and sintered states of MgO extrudate. The ultrasonic velocity and the AU (pulse amplitude, pulse width and ringdown count) measurements were reproducible within 1.5% and 10% respectively.

Except for anomalous decreases in porosity and velocity with respect to the green state in the early stages of sintering, which was attributed to pore growth, these parameters increased with the degree of sintering, i.e. increased as the sintering temperature and/or time increased. The increase in velocity was accounted for by the increase in elastic properties as the porosity fell during sintering.

Unlike velocity, which was largely determined by the percentage porosity, the AU parameters were sensitive to other microstructural features such as pore shape and size. Consequently, the changes in the AU parameters on sintering the extrudate were more complex and the pulse amplitude (PA) followed different trends to the pulse width (PW) and the ringdown count (RDC). This was explained in terms of attenuation and scattering.

Empirical relationships between the acoustic parameters and porosity and compressive strength were determined. High degrees of correlation with coefficients of regression of 0.95 and better were obtained for the velocity–porosity relationships, which demonstrates the potential for the use of velocity measurements in NDE. The correlation of AU parameters with porosity and strength was not so satisfactory, particularly in the case of PA. Nevertheless it is considered that these methods, especially the simple

ringdown counting technique, are worthy of further consideration and that, with better knowledge, fuller characterization may be obtained by employing both US and AU rather than either method in isolation.

Acknowledgements

One of the authors (T.K.) gratefully acknowledges a grant from the Indonesia BPP Teknology Overseas Fellowship Programme. The authors thank Morgan Matroc Ltd for kindly supplying the MgO samples.

References

1. A. VARY, "Materials Analysis by ultrasonics" (Noyes Data Corporation, Park Ridge, New Jersey, USA, 1987).
2. T. KATHRINA and R. D. RAWLINGS, *Br. Ceram. Trans.* **95**(6) (1996) 233.
3. *Idem*, *J. Eur. Ceram. Soc*., in press.
4. R. A. ROBERTS, *Mater. Eva.* **46** (1988) 758.
5. K. YAMANAKA, S. K. JEN, C. NERON and J. F. BUSSIERE, *ibid.* **47** (1989) 828.
6. M. ARNOULD, F. DUVANT, J. DU MOUZA and R. STRUILLOU, "Use of ultrasonic waves for the continuous control of microcracking in hot ceramics during drying, firing and cooling", Proceedings of the Final Contractor Meeting of EEC Research Development Programme in the Raw Material Sector in the area of Technical Ceramics (Elsevier, 1988) 281.
7. S. J. KLIMA and G. Y. BAAKLINI, in "Materials Analysis by Ultrasonics", edited by A. Vary (Noyes Data Corporation, Park Ridge, New Jersey, USA, 1987).
8. A. VARY, *Mater. Eva.* **40** (1982) 650.
9. K. K. PHANI, S. K. NIYOGI, A. K. MAITRA and R. ROYCHAUDHURY, *J. Mater. Sci.* **21** (1986) 4335.
10. A. O. B. ADUDA and R. D. RAWLINGS, "Acousto-ultrasonic testing of inorganic composites", presented at the 7th CIMTEC World ceramic congress, Montecaniti Terme, Italy (1990); Proceedings to be published by Elsevier.
11. A. C. DAS, S. K. NIYOGI and S. MUKHERJEE, *J. Mater. Sci. Lett.* **10** (1991) 173.
12. I. THOMPSON and R.D. RAWLINGS, *J. Mater. Sci.* **26** (1991) 4534.
13. S. SOMIYA, "Advanced Technical Ceramics" *Powder Technol.* (Academic Press, Japan, 1984).
14. O. J. WHITTEMORE, *Powder Technol.* **29** (1981) 167.
15. A. O. B. ADUDA and R. D. RAWLINGS, *J. Mater. Sci.* **29** (1994) 2297.
16. *Idem*, *Br. Ceram. Trans.* **95** (1996) 10.
17. J. SUMMERSCALES, "Non-destructive testing of fibre-reinforced plastics composites" (Elsevier Applied Science, London, New York, 1990).
18. A. VARY, in "Non-destructive Testing on fibre-reinforced plastics composites", edited by J. Summerscales (Elsevier Applied Science, London, New York, 1990) pp. 1–54.
19. C. B. SCRUBY and R. COLBROOK, *Br. J. NDT* **34** (3) (1992) 109.
20. R. HALMSHAW, "Non-destructive Testing" (Edward Arnold, London, 1987).

Received 5 November
and accepted 18 December 1996